Largely Enhanced Dielectric Constant of PVDF Nanocomposites through a Core-Shell Strategy

Minhao Yang[a], Hang Zhao[b], Chaohe Hu[a], Paul Haghi-Ashtiani[a], Delong He[, a], Zhi-Min Dang[c], Jinbo Bai*[, a]*

[a]Laboratoire de Mécanique des Sols, Structures et Matériaux, CNRS UMR 8579, Centrale-Supélec, Université Paris-Saclay, 3 Rue Joliot Curie, Gif-sur-Yvette, 91190, France

[b]State Key Lab Incubation Base of Photoelectric Technology and Functional Materials, International Collaborative Center on Photoelectric Technology and Nano Functional Materials, Northwest University, Xi'an 710069, People's Republic of China

[c]Department of Electrical Engineering, Tsinghua University, Beijing 100084, People's Republic of China

**Corresponding author.*

E-mail addresses: jinbo.bai@centralesupelec.fr (J. Bai)

delong.he@centralesupelec.fr (D. He)

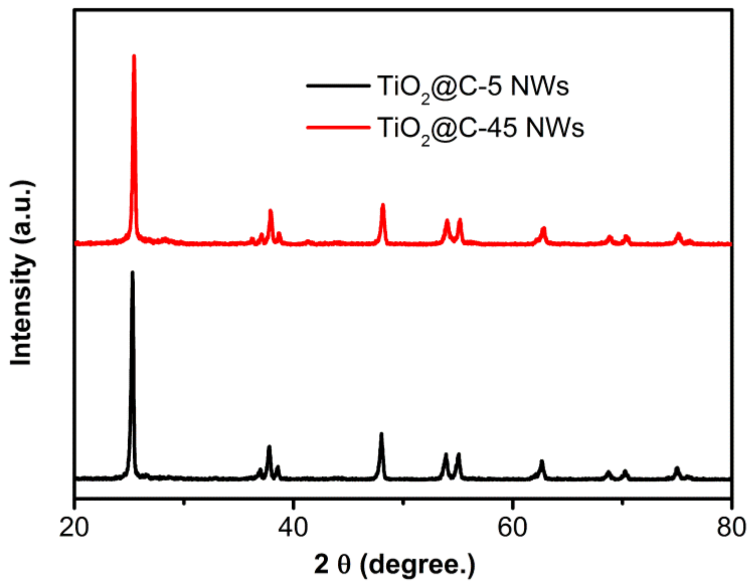

Fig. S1 XRD patterns of TiO_2@C NWs hybrids with different carbon shell thickness.

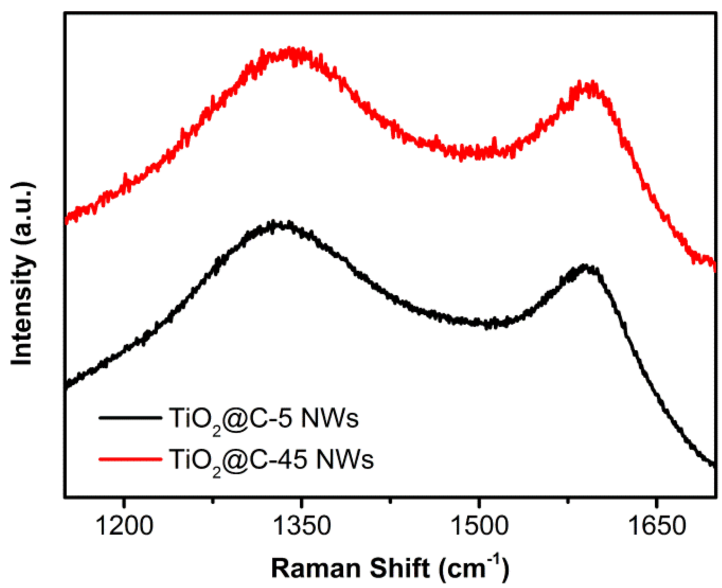

Fig. S2 Raman spectra of TiO_2@C NWs hybrids with different carbon shell thickness.

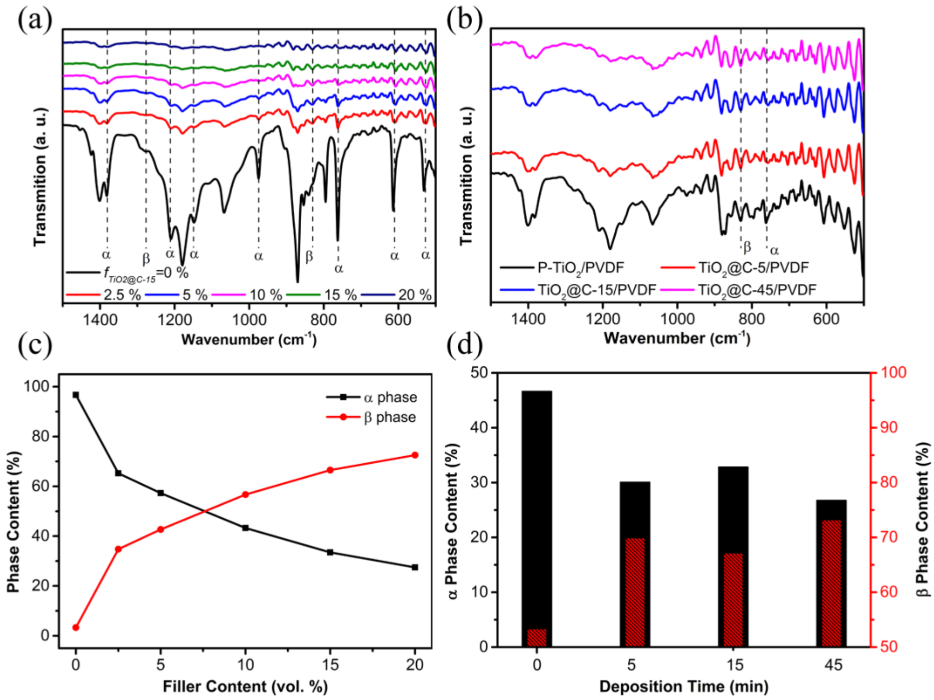

Fig. S3 FT-IR spectra of (a) PVDF and TiO_2@C-15 NWs/PVDF nanocomposites with different filler loadings and (b) TiO_2 NWs/PVDF and TiO_2@C NWs/PVDF nanocomposites with different hybrids at the same filler loading (15 vol. %); (c) The calculated relative content of α and β phase in PVDF and TiO_2@C-15 NWs/PVDF nanocomposites as a function of filler loading; (d) The calculated relative content of α and β phase in TiO_2 NWs/PVDF and TiO_2@C NWs/PVDF nanocomposites at 15 vol. % filler loading as a function of CVD time.

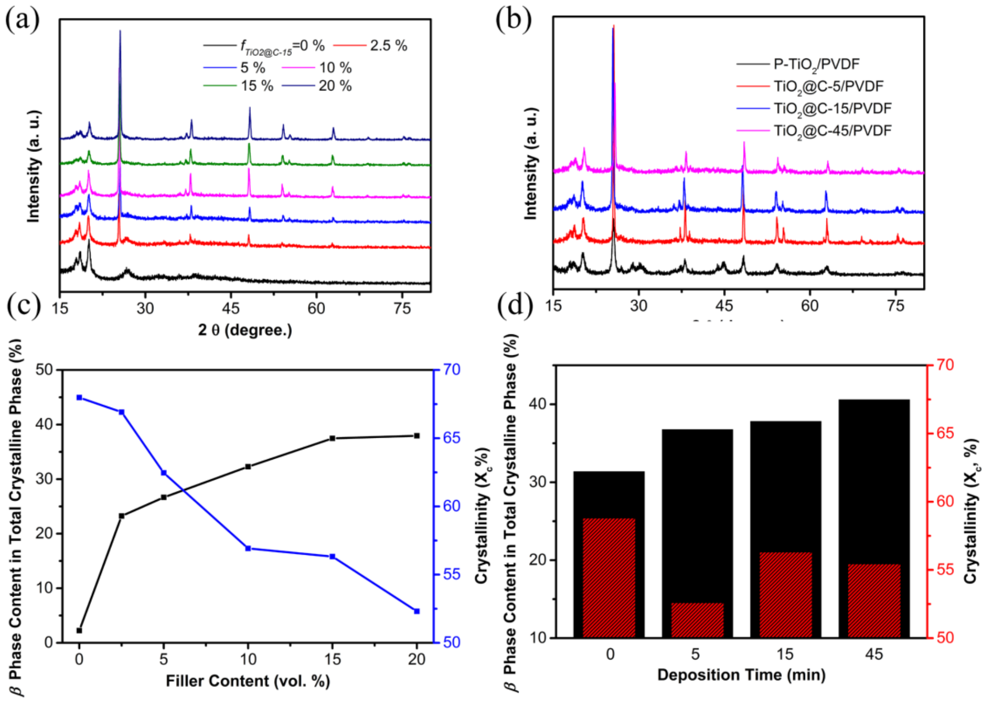

Fig. S4 XRD patterns of (a) PVDF and TiO_2@C-15 NWs/PVDF nanocomposites with different filler loadings and (b) TiO_2 NWs/PVDF and TiO_2@C NWs/PVDF nanocomposites with different hybrids at the same filler loading (15 vol. %); (c) The calculated content of β phase in total crystalline phase of PVDF and TiO_2@C-15 NWs/PVDF nanocomposites as a function of filler loading; (d) The calculated content of β phase in total crystalline phase of TiO_2 NWs/PVDF and TiO_2@C NWs/PVDF nanocomposites at 15 vol. % filler loading as a function of CVD time.

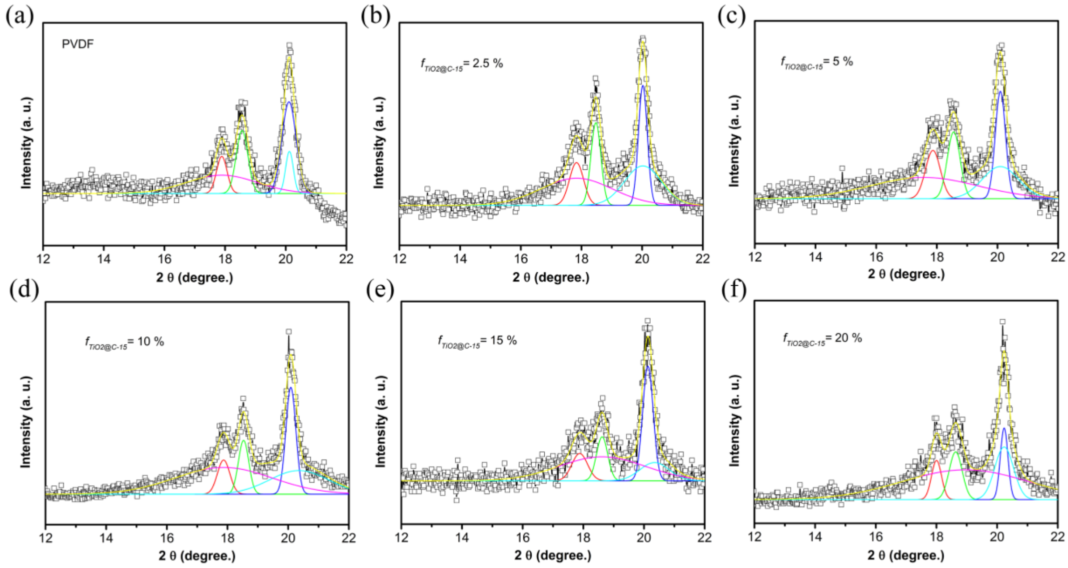

Fig. S5 Origin's multiple peak separation fitting results of PVDF and TiO_2@C-15 NWs/PVDF nanocomposites with different filler loadings.

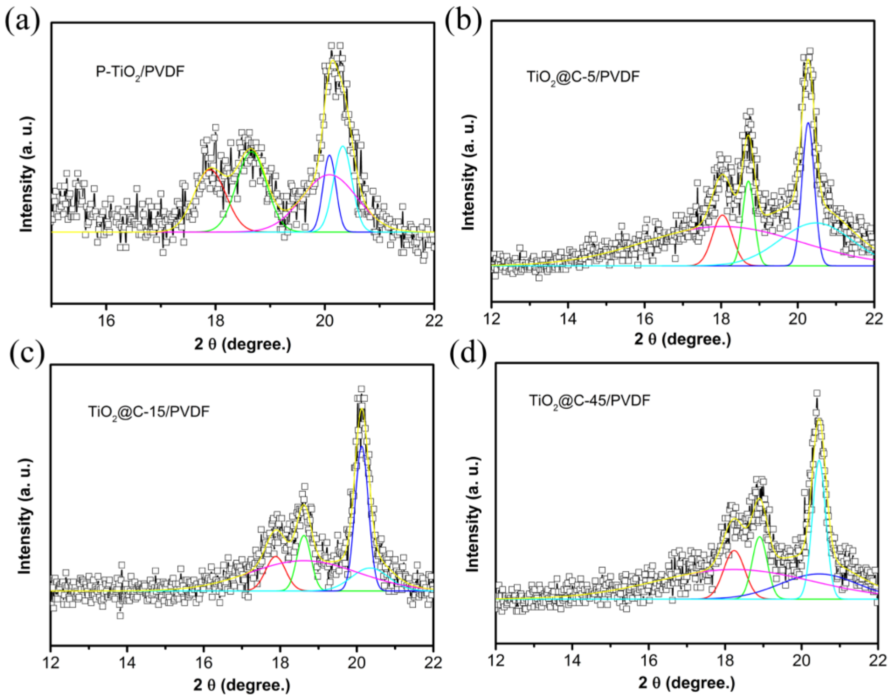

Fig. S6 Origin's multiple peak separation fitting results of TiO_2 NWs/PVDF and TiO_2@C NWs/PVDF nanocomposites with different hybrids at the same filler loading (15 vol. %).

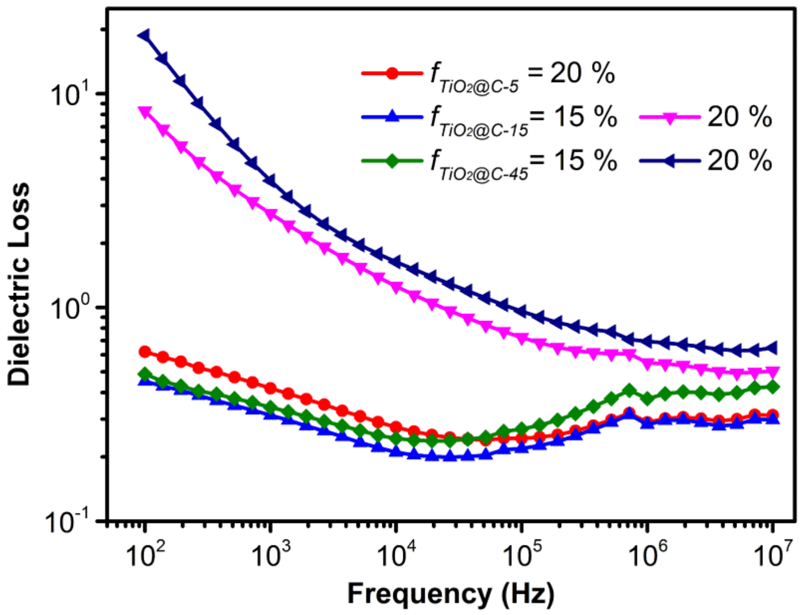

Fig. S7 Frequency dependence of the dielectric loss values of TiO_2@C-5 NWs/PVDF, TiO_2@C-15 NWs/PVDF and TiO_2@C-45 NWs/PVDF nanocomposites at different filler loadings.

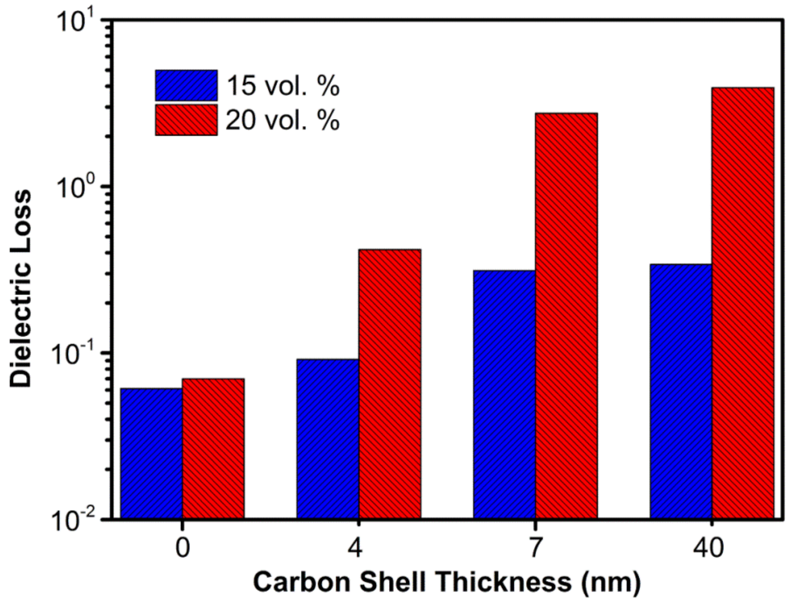

Fig. S8 Typical variation of dielectric loss values (10^3 Hz) of TiO_2 NWs/PVDF, TiO_2@C-5 NWs/PVDF, TiO_2@C-15 NWs/PVDF, and TiO_2@C-45 NWs/PVDF nanocomposites as a function of carbon shell thickness at different filler loadings (15 vol. % and 20 vol. %).

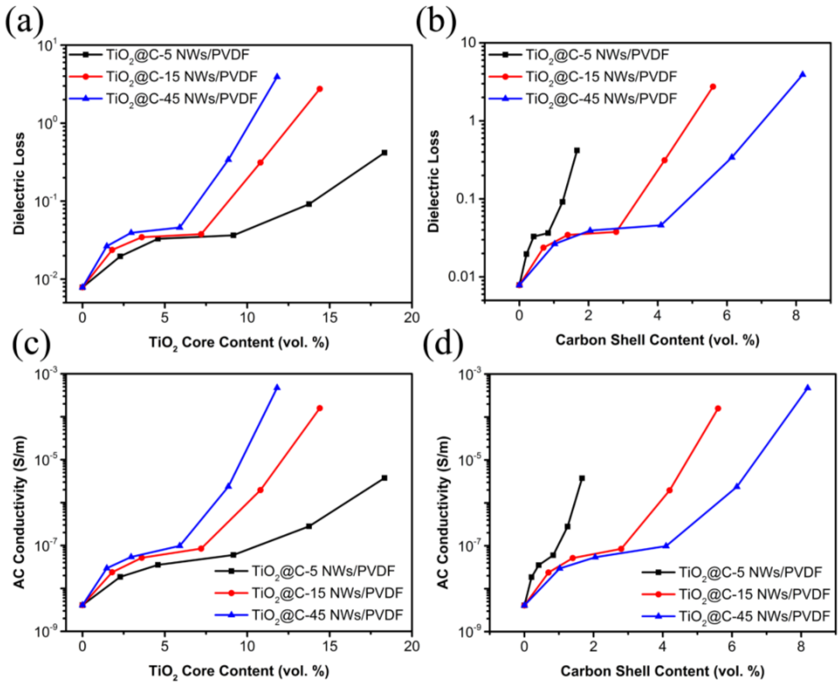

Fig. S9 Dependence of the dielectric loss and AC conductivity of TiO_2@C-5 NWs/PVDF, TiO_2@C-15 NWs/PVDF, and TiO_2@C-45 NWs/PVDF nanocomposites on the volume fraction of the TiO_2 NWs core and carbon shell for the whole nanocomposites (10^3 Hz).

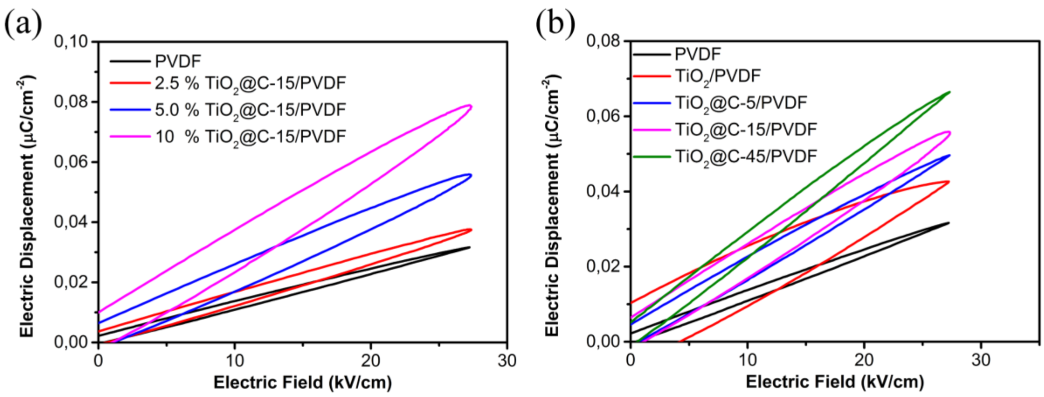

Fig. S10 The D-E loops of (a) PVDF and TiO_2@C-15 NWs/PVDF nanocomposites with different filler loadings (b) TiO_2 NWs/PVDF and TiO_2@C NWs/PVDF nanocomposites with different hybrids at the same filler loading (5 vol. %) at 10 Hz.

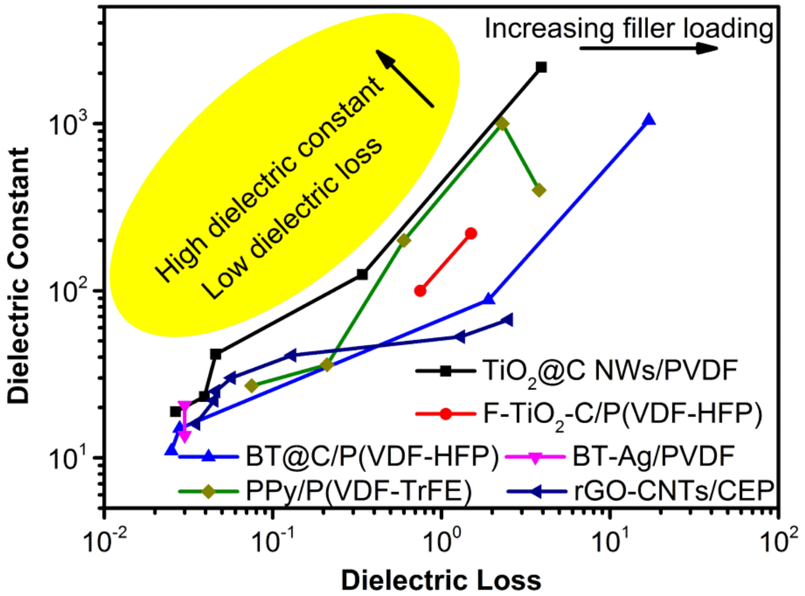

Fig. S11 Comparison of dielectric properties (10^3 Hz) of percolative nanocomposites with different types of nano-fillers: **TiO_2@C NWs**, 2.5-20 vol. %; **Flower-like TiO_2-C**, 15 and 20 vol. %; **BT@C,** 5-30 vol. %; **BT-Ag**, 7.6 and 18 vol. %; **PPy nanoclips**, 3-9 wt. %; **rGO-CNTs**, 0.02-0.144 wt. % **[1, 2, 3, 4, 5]**.

The derivation process of volume fraction of carbon shell (α):

The volume fraction of carbon shell in the hybrids (α) could be calculated from the weight fraction of carbon shell (β) as described below. The weight fraction of carbon shell in the hybrids could be obtained from the TGA curves. The equation for the calculation of α could be expressed as below.

$$\alpha = \frac{V_c}{V_h} = \frac{V_c}{V_c + V_{TiO2}} = \frac{\beta\, M/\rho_c}{\beta\, M/\rho_c + (1-\beta)M/\rho_{TiO2}} = \frac{\beta/\rho_c}{\beta/\rho_c + (1-\beta)/\rho_{TiO2}}$$

where V_c, V_{TiO2}, and V_h are the volume of carbon shell, TiO_2 core, and hybrids, respectively. The ρ_c and ρ_{TiO2} represent the density of carbon shell and TiO_2 core, respectively, and M is the mass of hybrids. The ρ_c and ρ_{TiO2} values are selected as 2.00 g cm^{-3} and 3.90 g cm^{-3}, respectively. The β is directly extracted from the TGA results.

Then the corresponding numerical values are put into the above-mentioned equation, and then the corresponding α could be obtained. The α for the TiO_2@C-5 NWs, TiO_2@C-15 NWs, and TiO_2@C-45 NWs are 8.34 %, 27.99 %, and 40.95 %, respectively.

1 L. Zhang, Z. Liu, X. Lu, G. Yang, X. Zhang and Z. Y. Cheng, *Nano Energy*, 2016, **26**, 550-557.

2 S. Luo, S. Yu, R. Sun and C. P. Wong, *ACS Appl. Mater. Interfaces*, 2013, **6**, 176-182.

3 Y. Feng, W. Li, J. Wang, J. Yin and W. Fei, *J. Mater. Chem. A.*, 2015, **3**, 20313-20321.

4 N. Xu, Q. Zhang, H. Yang, Y. Xia and Y. Jiang, *Sci. Rep.*, 2017, **7**, 43970.

5 J. Y. Kim, T. Kim, J. W. Suk, H. Chou, J. H. Jang, J. H. Lee, I. N. Kholmanov, D. Akinwande and R. S. Ruoff, *Small*, 2014, **10**, 3405-3411.